



# Numerical Analysis to Enhance Delamination Strength around Bolt Holes of Unidirectional Pultruded Large Smart Composite Platform

Sheedev Antony, Monssef Drissi Habti, Venkadesh Raman

## ► To cite this version:

Sheedev Antony, Monssef Drissi Habti, Venkadesh Raman. Numerical Analysis to Enhance Delamination Strength around Bolt Holes of Unidirectional Pultruded Large Smart Composite Platform. *Advances in Materials Science and Engineering*, 2018, 2018, pp.3154904. 10.1155/2018/3154904 . hal-04441715

**HAL Id: hal-04441715**

**<https://hal.science/hal-04441715>**

Submitted on 6 Feb 2024

**HAL** is a multi-disciplinary open access archive for the deposit and dissemination of scientific research documents, whether they are published or not. The documents may come from teaching and research institutions in France or abroad, or from public or private research centers.

L'archive ouverte pluridisciplinaire **HAL**, est destinée au dépôt et à la diffusion de documents scientifiques de niveau recherche, publiés ou non, émanant des établissements d'enseignement et de recherche français ou étrangers, des laboratoires publics ou privés.



Distributed under a Creative Commons Attribution 4.0 International License

## Research Article

# Numerical Analysis to Enhance Delamination Strength around Bolt Holes of Unidirectional Pultruded Large Smart Composite Platform

Sheedev Antony, Monssef Drissi-Habti , and Venkadesh Raman

*PRES LUNAM IFSTTAR, CS4 Route de Bouaye, 44344 Bouguenais, France*

Correspondence should be addressed to Monssef Drissi-Habti; [monssef.drissi-habti@ifsttar.fr](mailto:monssef.drissi-habti@ifsttar.fr)

Received 10 January 2018; Accepted 29 April 2018; Published 27 June 2018

Academic Editor: Julian Wang

Copyright © 2018 Sheedev Antony et al. This is an open access article distributed under the Creative Commons Attribution License, which permits unrestricted use, distribution, and reproduction in any medium, provided the original work is properly cited.

As a part of the DECID2 French National Project (2008–2012), construction of a large platform entirely made of smart composites was carried out and two demonstrators were installed. During a previous study, an ABAQUS model of smart composite platform was set up to perform numerical simulations that predict the mechanical behaviour of bolt-fastened platform under static three-point bending load, and a stress concentration is observed around the bolt holes. Unidirectional composites are subjected to delamination at very low stress, and this cannot be tolerated because most of the applications of pultruded structures are in civil engineering, which involves human safety. Therefore, it is essential to study the correlation of delamination onset and find a technology to enhance delamination strength. In this study, a numerical analysis was carried out to enhance the delamination strength around the bolt holes. Bidirectional fiberglass cloths were wrapped around unidirectional pultruded beams to reinforce the structure and to prevent delamination. Due to the high cost of these cloths, a study was also carried out to select an appropriate cloth material by taking into account two aspects: density and number of layers of cloths. The selected cloth was compared with conventional continuous fibreglass mat, and it was found that bidirectional fibreglass cloth material performs well in preventing delamination, even though it is expensive.

## 1. Introduction

Fiber-reinforced polymer composites are materials that are composed of polymer-based resin and fibres as reinforcement. Composite material properties are mainly determined based on fibres and resin properties, fibre volume fraction, and geometry and orientation of fibres. Utilization of polymer matrix composites is increasing day by day in many industries due to their better mechanical properties, corrosion resistance, and strength-to-weight ratio, but their durability remains an issue. The introduction of smart composite material structures with structural health monitoring (SHM) techniques is one solution to these problems. In SHM, sensors will detect strain at different locations of composite structures and monitor the health of the structure. The detailed studies of smart composite materials are discussed in the previous work [1].

The main goal of DECID2 project (2008–2012) was the construction of mechanically oriented platforms made of pultruded composite materials (Figure 1). Two demonstrators of dimensions  $20\text{ m} \times 3.5\text{ m}$  were installed in IFSTTAR Nantes and Technocampus EMC2. The parts were attached using single and double lap-bolted joints. Different studies were carried out to reduce delamination and to study the behaviour of bolted joints in composite structures [2, 3]. It was found that high-speed drilling and low feed rates may reduce the intensity of delamination [2], but DECID2 project has been started prior to the publishing of these studies, and conventional drilling methods were used during construction. Strain sensors and ultrasonic sensors were embedded in pultruded composite structures. This technique is called structural health monitoring where strain will be continuously monitored and warned when it reaches the strain limit. Several possible sensors for monitoring large smart composite



FIGURE 1: DECID2 platform.

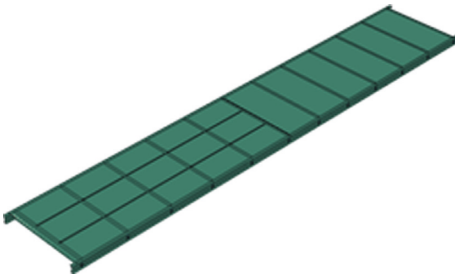


FIGURE 2: Smart composite platform CAD model [7].

structure have been studied previously [4, 5], and further works were extended to the study of UV radiation defect on mechanical behaviour of the DECID2 smart composite platform [6]. For further studies, a CAD model of large smart composite platform was set up, and a numerical simulation to predict the mechanical behaviour of the structure under static load has been performed (Figure 2). As a result of this work, it was observed that there was a stress concentration around bolt holes (Figure 3) [7].

Pultrusion is a continuous manufacturing process of composite materials with constant cross sections. In this technology, parts are made by the matrix extrusion process and by pulling the unidirectional fibres. This process will allow the fibres to align well before polymerization of the matrix. It is a highly automated, cost-effective process and produces finished parts with high volume fraction. Pultrusion is used to make products like beams, pipes, and tubes, which are used in civil structures like bridges, light poles, and towers (Figure 4) [8].

But in many cases, unidirectional composites are subjected to delamination at very low stress, and these issues cannot be tolerated in some demanding applications. In [11], it is mentioned that debonding (Figure 5) occurs prior to other local defects, and this will lead to delamination (Figure 6). As mentioned earlier, most of the applications of pultruded materials are in civil engineering industries, which involve human safety. Therefore, it is essential to study the correlation of delamination onset and find a technology to enhance delamination strength as high as possible. In this technology, unidirectional composite will be wrapped with bidirectional fiberglass cloth with appropriate density and number of layers, which can enhance the delamination strength and decrease the risk of catastrophic failure of the structure. In order to validate the use of bidirectional fiberglass cloth over the cheap continuous fiberglass mat, a comparative study will be also carried out.

The aim of this work is to suggest a technique to enhancing delamination strength around bolt holes of unidirectional

pultruded composite. All the experimental validation tests of the platform have been carried out, except those relating to the local analysis of stainless steel-bolted joints. Indeed, we were forced to complete the project in the allotted time, and there remain some scientific and technological points to complete numerically. Experimental validation is unfortunately no longer possible because the composite material platform is already manufactured and cannot be dismantled for testing. In this paper, we have performed a numerical analysis of the assembly areas, and we have demonstrated numerically how these areas could be reinforced by fiberglass fabrics. On the one hand, the innovation lies more in the proposal of the concept of local extra thickness to be applied to the zones of assemblies, and on the other hand, the calculations made it possible to optimize the type and the density of fibreglass fabrics. Our assumptions are strongly below the critical threshold of matrix cracking. We have therefore taken into account this mechanism which is even the source of this work. Firstly, a composite micromechanical model will be set up in ABAQUS. The bi-directional fibreglass cloth wrapping method (Figure 7) will be used to reduce delamination around bolt holes, and this method will be validated. Due to the high cost of bidirectional fibreglass cloths, a study will also be carried out to select an appropriate cloth material by taking into account two aspects: density and number of layers of cloths. The selected bi-directional fibreglass cloths will be compared with conventional continuous fiberglass mat to evaluate the difference in damage reduction performance.

## 2. Technology Proposed and Numerical Modelling

**2.1. Wrapping Technology.** In the wrapping technique, unidirectional pultruded beams will be wrapped using bi-directional fiberglass cloths or continuous fiberglass mats. In this study, thin bidirectional fiberglass cloths with E-glass vinylester material was used due to their better mechanical properties (Tables 1 and 2). The orientation of bidirectional fiberglass cloths will be set to  $0^\circ$  and  $90^\circ$ , and thicknesses will be scaled down for the following simulations.

Bolted joint fasteners and drilling method are the most commonly used techniques in composite structure to join parts. While drilling a unidirectional pultruded composite structure (Figure 8), the fibres will start to separate near the bolt holes and this will lead to a huge defect in the whole structure. The separation will start from the interface between fibre and matrix, which is called debonding. This debonding in microscale will lead to delamination, and it is very essential to avoid or decrease the intensity of this defect. This fibre separation can be reduced to an extent by wrapping these unidirectional pultruded fibres using bidirectional fiberglass cloths. This will reinforce composite structure and protect them from delamination by holding unidirectional fibres together. Bidirectional fiberglass cloth will also allow the structure to be reinforced in both directions while it was before reinforced in unidirectional only.

**2.2. Micromechanical Model.** To study delamination, a composite micromechanical model of pultruded unidirectional

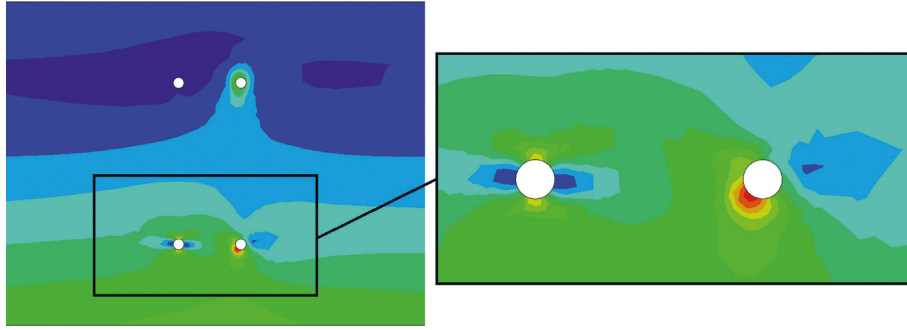


FIGURE 3: Stress concentration around the bolt holes (red contour indicating high stress) [7].

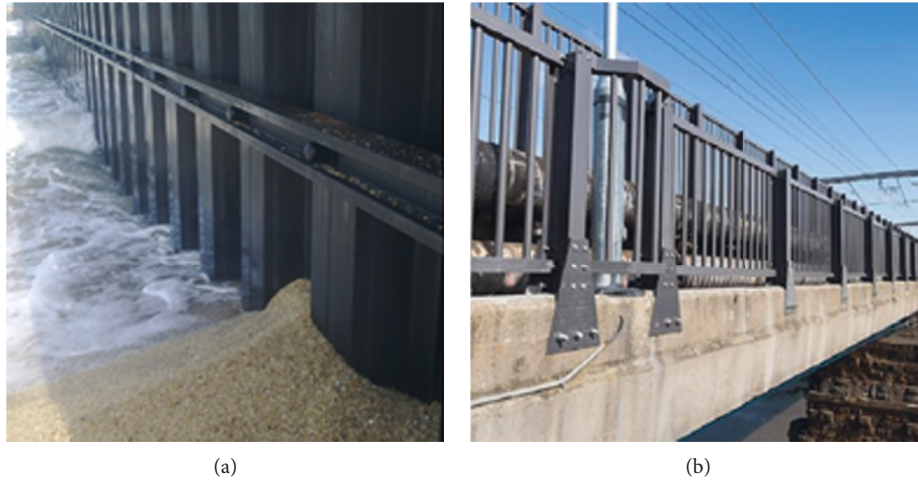


FIGURE 4: Pultruded retaining wall in Azerbaijan (a) and pultruded railway bridge barriers in England (b) [9, 10].

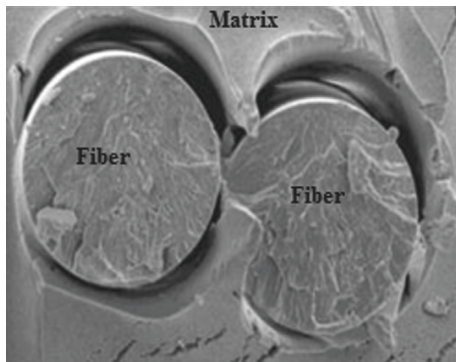


FIGURE 5: Fiber-matrix debonding [12].

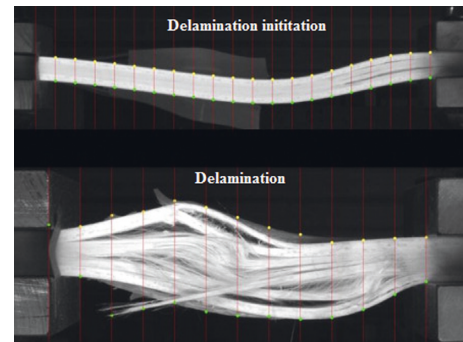


FIGURE 6: Delamination [13].

material with a hole was set up (Figure 9). This model is just a representation of composite structure with a hole that was cut through the fibres. The material properties assigned were E-glass and vinylester (Tables 3 and 4). The diameter of the fibres were 0.014 mm, and size of the micromechanical model was  $0.06 \text{ mm} \times 0.06 \text{ mm} \times 0.06 \text{ mm}$ . Fibre volume fraction is considered as around 66% (pultrusion). Fibres and matrix were created separately and assembled together. Cohesive surface contact (interface) properties were assigned between fibres and matrix.

**2.3. Theoretical Considerations of Interaction Properties.** Surface-based cohesive behaviour allows the specification of generalized traction-separation behaviour for surfaces. This behaviour was offering capabilities that are very similar to the cohesive elements, which were defined using traction-separation law, and it requires only less computational time compared with cohesive element in ABAQUS. Surface-based cohesive behaviour was very easy to define, and it allows the simulation of a wider range of cohesive interactions. This method was very useful in this analysis because the surfaces



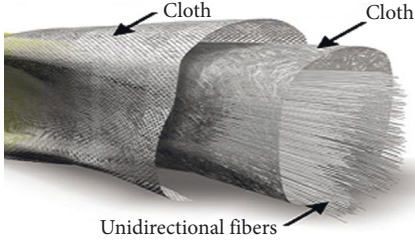


FIGURE 7: Bidirectional E-glass cloth and unidirectional E-fiber-glass [14].

TABLE 1: Properties of E-glass vinylester bidirectional fiberglass composite [15].

| Parameter (unit)             | E-glass vinylester bidirectional |
|------------------------------|----------------------------------|
| Density (kg/m <sup>3</sup> ) | 1988                             |
| $E_1$ (MPa)                  | 20,769                           |
| $E_2$ (MPa)                  | 20,769                           |
| $\nu_{12}$                   | 0.09                             |
| $G_{12}$ (MPa)               | 4133                             |
| Thickness (mm)               | 0.1                              |

TABLE 2: Parameters for damage analysis of E-glass vinylester bidirectional fiberglass composite [15].

| Parameter (unit)                        | Notation | Value |
|---|----------|-------|
| Longitudinal tensile strength (MPa)     | $X_T$    | 395   |
| Longitudinal compressive strength (MPa) | $X_C$    | 260   |
| Transverse tensile strength (MPa)       | $Y_T$    | 395   |
| Transverse compressive strength (MPa)   | $Y_C$    | 260   |
| Longitudinal shear strength (MPa)       | $S_L$    | 75    |
| Transverse shear strength (MPa)         | $S_T$    | 75    |
| Cross product term coefficient          |          | -0.5  |
| Stress limit                            |          | 0     |

were in contact (fibre and matrix), and there were no interface thicknesses.

Nominal traction stress vector  $t$  is a combination of three components:  $t_n$ ,  $t_s$ , and  $t_t$  which represent the normal and two shear tractions, respectively. The corresponding separations are denoted by  $\delta_n$ ,  $\delta_s$ , and  $\delta_t$ . And cohesive element thickness is defined as  $T_0$ . Nominal strain can be written as

$$\epsilon_n = \frac{\delta_n}{T_0} \quad \epsilon_s = \frac{\delta_s}{T_0} \quad \epsilon_t = \frac{\delta_t}{T_0}. \quad (1)$$

Elastic behaviour can be represented by

$$t = \begin{Bmatrix} t_n \\ t_s \\ t_t \end{Bmatrix} = \begin{bmatrix} k_{nn} & k_{ns} & k_{nt} \\ k_{sn} & k_{ss} & k_{st} \\ k_{tn} & k_{ts} & k_{tt} \end{bmatrix} \begin{Bmatrix} \delta_n \\ \delta_s \\ \delta_t \end{Bmatrix}. \quad (2)$$

Damage modelling was helpful to simulate degradation and eventual failure of the bond between two cohesive surfaces. The failure mechanism in surface-based cohesive behaviour consists of two parameters:

- (i) Damage initialization criterion
- (ii) Damage evolution law

Damage will evolve according to the damage evolution law after damage initiation criterion is met. A quadratic stress damage initiation criterion and an energy damage evolution law are defined. The graph (Figure 10) shows the typical traction-separation response with a failure mechanism. The damage was assumed to initiate when a quadratic interaction function involving the separation ratios reaches a value of one. This criterion can be represented as

$$\left\{ \frac{\langle t_n \rangle}{t_n^0} \right\}^2 + \left\{ \frac{\langle t_s \rangle}{t_s^0} \right\}^2 + \left\{ \frac{\langle t_t \rangle}{t_t^0} \right\}^2 = 1, \quad (3)$$

where  $t_n$ ,  $t_s$ , and  $t_t$  are the contact stress normal to the interface along first and second shear directions, respectively;  $t_n^0$ ,  $t_s^0$ , and  $t_t^0$  are the peak values of contact stress when separation is either purely normal to interface or purely in the first or second shear direction, respectively; and  $\langle \cdot \rangle$  is the Macaulay bracket indicating that a purely compressive stress state does not initiate damage.

Damage evolution was assigned based on the energy. Simplest way to define the fracture energy was to specify it directly as a function of the mixed mode in tabular form. Fracture energy  $G_c$  is equal to the area under the traction-separation curve. The tie contact interaction was used to attach bidirectional fiberglass cloths to micromechanical model of unidirectional pultruded composite [16].

The cohesive elements are modelled as undergoing progressive damage leading to failure and the progressive damage modelling involves softening in the material response, which can lead to convergence difficulties in an implicit solution procedure: ABAQUS/Standard. In order to avoid these convergence issues, ABAQUS/Standard provides a viscous regularization capability that helps in improving the convergence. The use of viscous regularization of the constitutive equations causes the tangent stiffness matrix of the softening material to be positive for sufficiently small time increments [17].

In this study, traction-separation laws are regularized in ABAQUS/Standard using viscosity by permitting stresses to be outside the limits set by the traction-separation law, and this regularization process involves the use of viscous stiffness degradation variable,  $D_v$ , which is defined by the following evolution equation:

$$\dot{D}_v = \frac{1}{\mu} (D - D_v), \quad (4)$$

where  $\mu$  is the viscosity parameter and  $D$  is the current damage.

For viscous material, the damage response is

$$t = (1 - D_v) \bar{t}. \quad (5)$$

Using viscous regularization with a small value of the viscosity parameter (small compared to the characteristic time increment) usually helps in improving the rate of convergence of the model in the softening regime, without compromising results. The basic idea is that the solution of the viscous system relaxes into that of the inviscid case as  $t/\mu \rightarrow \infty$  where  $t$  represents time. The use of viscous regularization is a powerful and often necessary tool that enables accurate prediction of delamination, and this approach

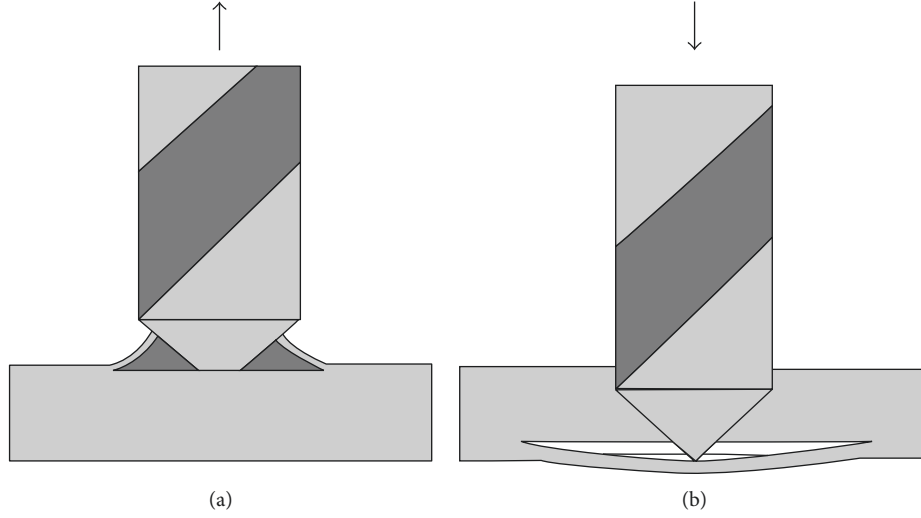


FIGURE 8: Schematic of delamination push-out at exit (a) and peel-up at the entry (b).

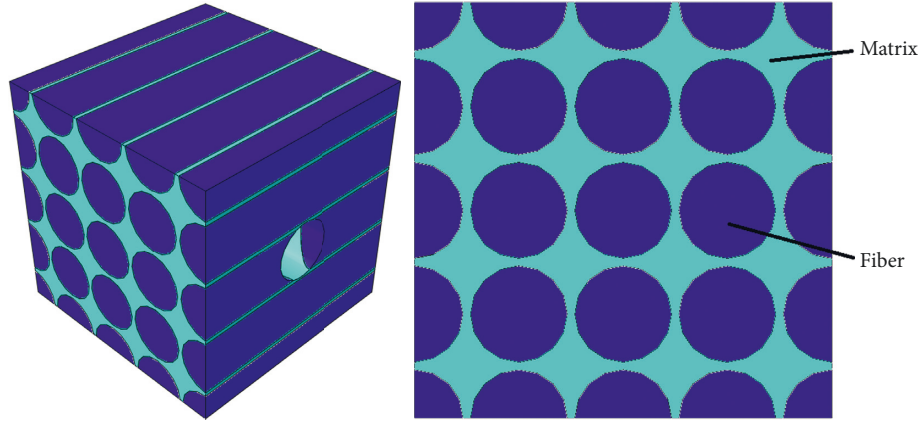


FIGURE 9: Composite micromechanical model.

TABLE 3: Properties of vinylester resin [11].

| Parameter (unit)                              | Vinylester |
|---|------------|
| Density ( $\text{g/cm}^3$ )                   | 1.05       |
| Poisson coefficient, $\nu$                    | 0.35       |
| Shear modulus (GPa)                           | 1.24       |
| <i>Tension</i>                                |            |
| Modulus, $E$ (GPa)                            | 3.2        |
| Tensile strength, $\sigma_{\text{ult}}$ (MPa) | 86         |
| <i>Compression</i>                            |            |
| Modulus, $E$ (GPa)                            | 3.35       |
| Yield strength, $\sigma_y$ (MPa)              | 103        |

is used here in order to improve the rate of convergence of the model [17, 18].

In this analysis, a global stabilization factor (dissipated energy fraction) of  $2 \times 10^{-4}$  was used to perform numerical analysis [19]. By adopting a weakening factor of  $f_w$  0.3, the interfacial strength properties were reduced from the matrix material [20–22] which indicate a relatively weak interface in pultruded glass fibre-reinforced material. The elastic stiffness (per unit area) of the interface was assumed to be equal to  $10^6 \text{ N/mm}^3$  [23]. The critical normal interface tractions

TABLE 4: Properties of E-fiberglass [15].

| Parameter (unit)                 | E-glass |
|----------------------------------|---------|
| Density ( $\text{g/cm}^3$ )      | 2.54    |
| Young's modulus in tension (GPa) | 73      |
| Tensile strength (MPa)           | 2400    |
| Compressive strength (MPa)       | 1450    |
| Shear modulus (GPa)              | 33.3    |
| Poisson coefficient, $\nu$       | 0.22    |
| Diameter ( $\mu\text{m}$ )       | 14      |

of the cohesive zone elements were equal to the normal tensile strength of the unidirectional layers in the direction normal to the fibres (Table 5), that is,  $13.5 \text{ N/mm}^2$ , and the critical shear interface tractions were equal to the unidirectional shear strength (Table 5), that is,  $13.5 \text{ N/mm}^2$ . For the pultruded material mode I, mode II, and mode III critical energy release rates  $G_{\text{Ic}}$  and  $G_{\text{IIc}} = G_{\text{IIIc}}$  were taken as  $0.2 \text{ N/mm}$  and  $0.5 \text{ N/mm}$ , respectively [24]. The bi-directional fibreglass cloth was attached to the unidirectional micromechanical model using tie contact constraint in the four surfaces.

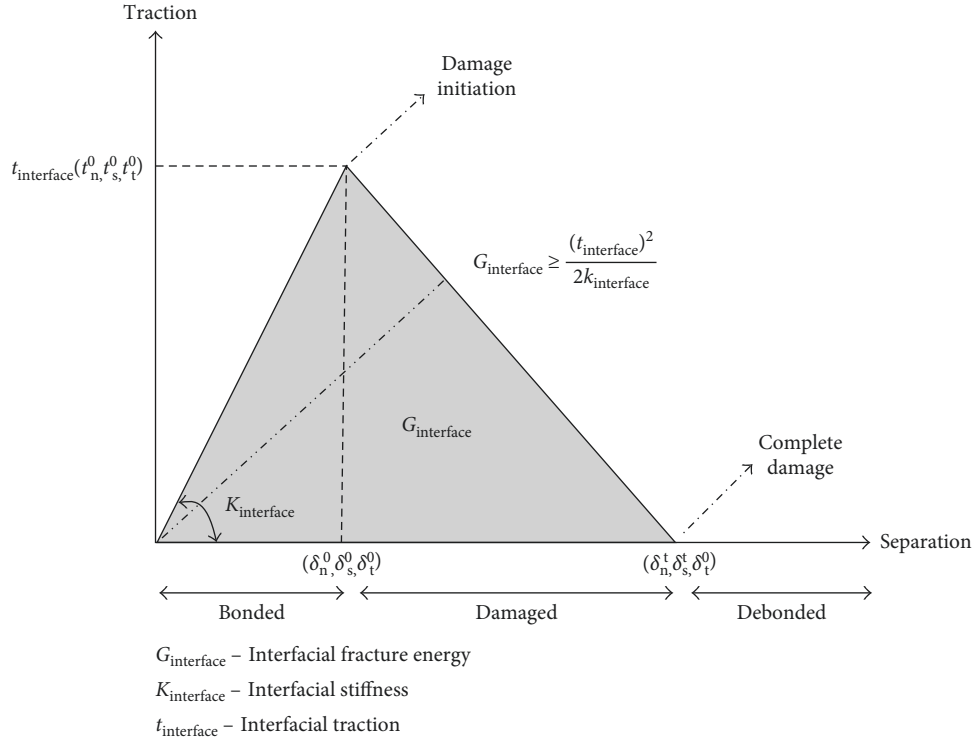


FIGURE 10: Typical traction-separation response [18].

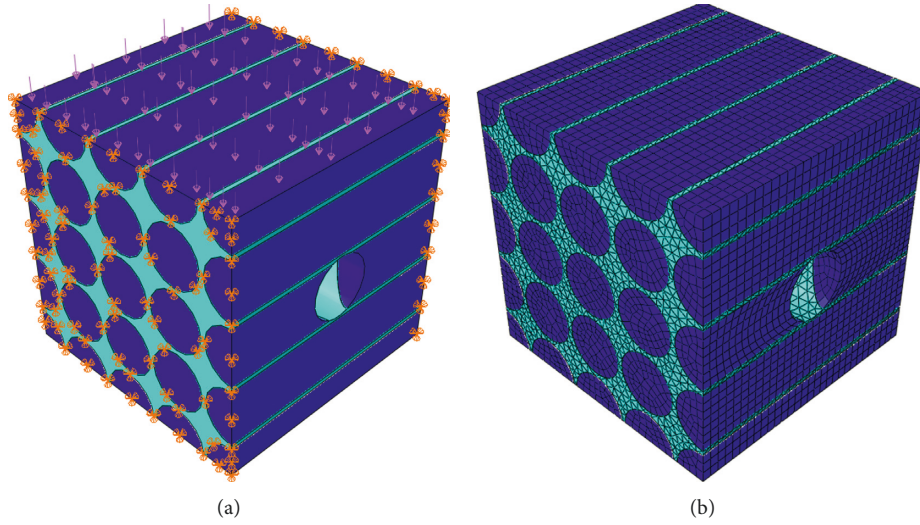


FIGURE 11: Load and boundary conditions (a) and mesh (b) on the composite micromechanical model.

**2.4. Load and Boundary Conditions and Mesh.** The micro-mechanical model was subjected to pressure force from the top. As the interest was to study delamination, left and right surfaces are constrained using the pinned join boundary condition that was allowing the material to delaminate easier and was comparatively easy for simulation convergence (Figure 11). This method of load and boundary conditions and mesh was maintained similar in all simulations that were carried out.

The parts of the model were meshed separately. Fibre was meshed using 26,664 C3D8R elements and matrix using 65,290 C3D10 elements. Cloth layer 1 was meshed using

TABLE 5: Parameters for damage analysis of E-glass vinylester unidirectional composite [16].

| Parameter (unit)                        | Notation | Value |
|---|----------|-------|
| Longitudinal tensile strength (MPa)     | $X_T$    | 1200  |
| Longitudinal compressive strength (MPa) | $X_C$    | 620   |
| Transverse tensile strength (MPa)       | $Y_T$    | 45    |
| Transverse compressive strength (MPa)   | $Y_C$    | 100   |
| Longitudinal shear strength (MPa)       | $S_L$    | 45    |
| Transverse shear strength (MPa)         | $S_T$    | 45    |
| Cross product term coefficient          |          | -0.5  |
| Stress limit                            |          | 0     |

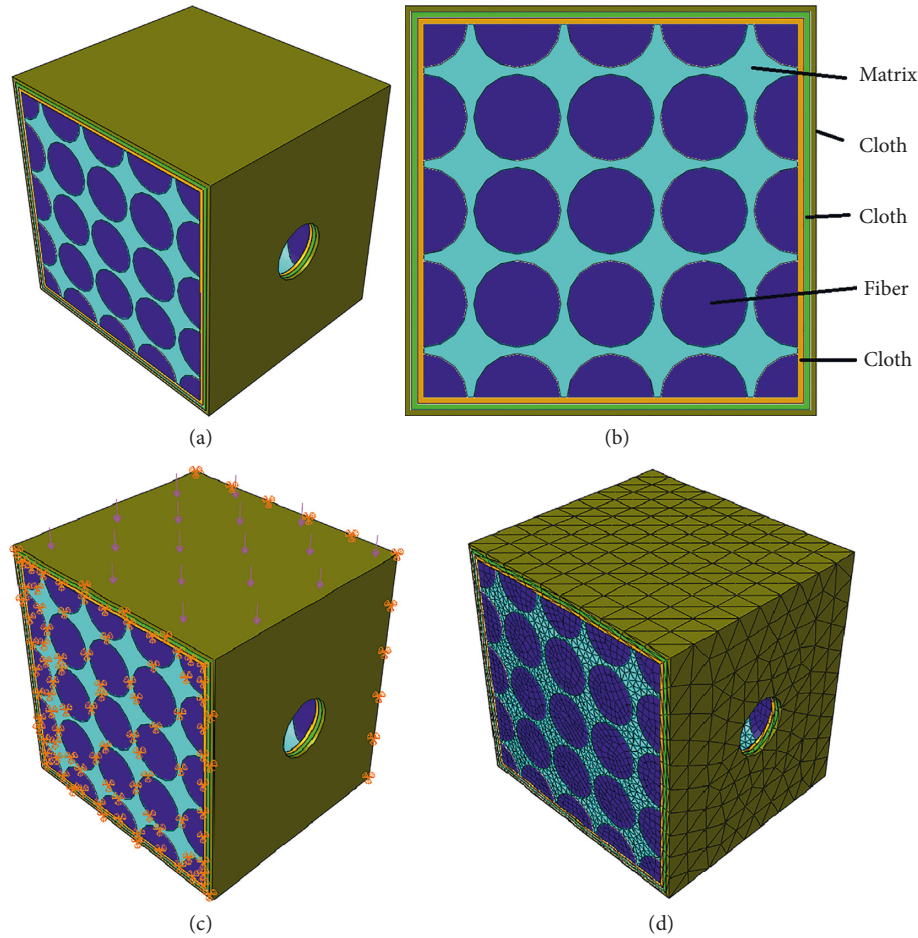


FIGURE 12: Composite micromechanical model: (a) isometric view; (b) front view; (c) load and boundary conditions; (d) mesh of composite micromechanical model with 3-layer cloth.

C3D10 2643 elements, cloth layer 2 was meshed using C3D10 2423 elements, and cloth layer 3 was meshed using 2494 C3D10 elements (Figure 12). Different simulations were performed using these composite micromechanical models to study the damage. (C3D8R: continuum 3-D, 8-node, reduced integration; C3D10: continuum 3-D, 10-node).

The bidirectional fiberglass cloths with different number of layers and densities were wrapped on the composite micromechanical model, and different simulations were performed. These simulations were carried out to select a better bidirectional fiberglass cloth, which can decrease stress concentration and damage. Due to the cost-effectiveness considerations and small thicknesses of beams, the appropriate number of layers of wraps and the better material selection were evident. Weight and thickness of the bidirectional fiberglass cloth chosen are shown in Table 6.

### 3. Results and Discussion

For comparison, numerical simulations were carried out without wrapping fiberglass cloths and with wrapping different layers of bidirectional fiberglass cloths. Damage initiation stress and interface damage occurring between fibre and matrix of each model were used for comparison.

TABLE 6: Weight and thickness of the bidirectional fiberglass cloth [25].

| Weight (g/m <sup>2</sup> ) | Thickness (mm) |
|----------------------------|----------------|
| 186                        | 0.14           |
| 295                        | 0.23           |
| 318                        | 0.28           |

**3.1. Micromechanical Model.** Stress contour plots obtained from different numerical simulations were plotted to visualize the performance of the model before and after wrapping different layers of bidirectional fiberglass cloths. Micromechanical models were subjected to high loads in order to study damage. Figure 13(a) shows stress contour plot of the micromechanical model before wrapping bidirectional fiberglass cloths. A maximum stress of 5344 MPa and fibre-matrix separation are observed in this model. Debonding is decreased in Figure 13(b) after addition of 1 layer of bidirectional fiberglass cloth. Bidirectional fiberglass cloth wrapping reinforced the model and decreased maximum stress to 3674 MPa. Similarly, maximum stress is decreased for 2 layer and 3 layer as shown in Figure 13(c), and maximum stress is also decreased to 3175 MPa and 2433 MPa, respectively, as shown in Figure 13(d). Maximum



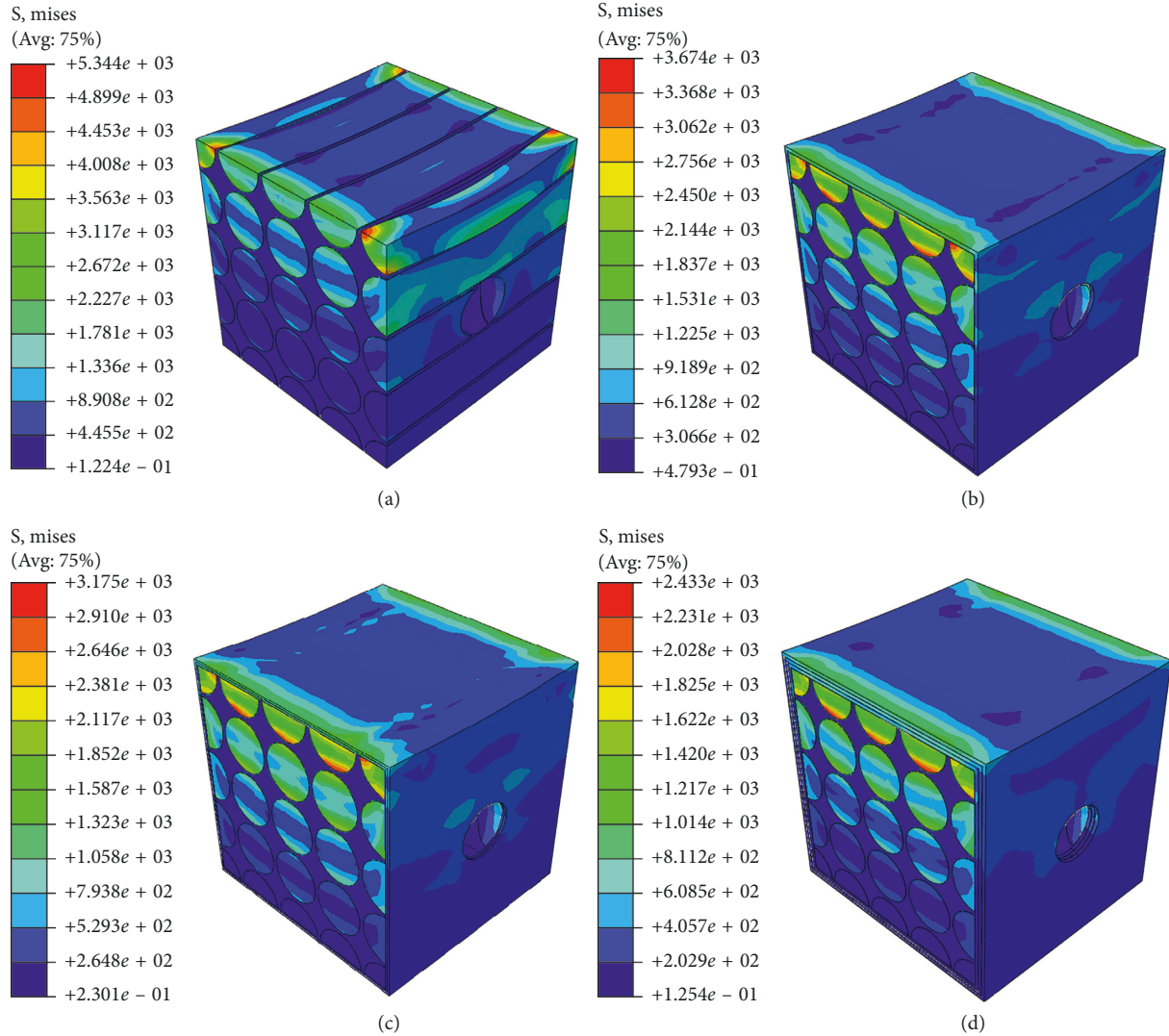


FIGURE 13: Stress on the composite micromechanical model: (a) without cloth; (b) with 1 layer cloth; (c) with 2 layer cloth; (d) with 3 layer cloth.

stresses were found near the fibre-matrix interface in all models, and addition of bidirectional fiberglass cloths results in decreasing of these stresses.

The result of stress versus damage obtained from different models was plotted together, and Figure 14 shows the behaviour of stress versus damage for each model. In the micromechanical model without cloth, damage initiation stress was estimated as 18 MPa. High interface damage and fibre-matrix debonding are observed in this model. In order to increase damage initiation stress, the micromechanical model is wrapped with one layer of bidirectional fiberglass cloth. After wrapping, fibre-matrix debonding is restricted and interface damage is decreased. As a result, damage initiation stress is increased to 23 MPa. Bidirectional fiberglass cloth wrapping has reduced fibre-matrix debonding by holding them together. Similarly, more bidirectional fiberglass cloths were wrapped, and damage initiation stress is increased to 28 MPa and 36 MPa for 2 layer and 3 layer of bidirectional fibre cloth wraps, respectively. It was observed that bidirectional fiberglass cloth wrapping assists fibre-matrix bonding to be stronger and reduces delamination,

which occurs around the bolt hole of the unidirectional pultruded model.

Considering Figure 14 into 2 areas, in Area 1, damage is initiated and stress is incrementing steadily from 16 MPa to 22 MPa for the model without cloth, 23 MPa to 51 MPa for 1-layer cloth, 28 MPa to 60 MPa for 2-layer cloth, and 34 MPa to 83 MPa for 3-layer cloth in the damage coefficient limit 0 to 0.8. The increase in the stress value near to damage coefficient 0.8 is due to starting of complete damage. In Area 2, huge variation in stress can be observed due to the complete damage to the models, and the difference in variation of the stress value for each model shows their restriction to damage. A model without cloth is fully damaged in less stress limit comparatively, and after adding bidirectional fiberglass cloths, damage is restricted and stress required for complete damage is extended for each layer.

### 3.2. Effect of Bidirectional Fiberglass on Platform Model.

The micromechanical analysis provided an evident result of the impact of wrapping bidirectional fiberglass cloths on

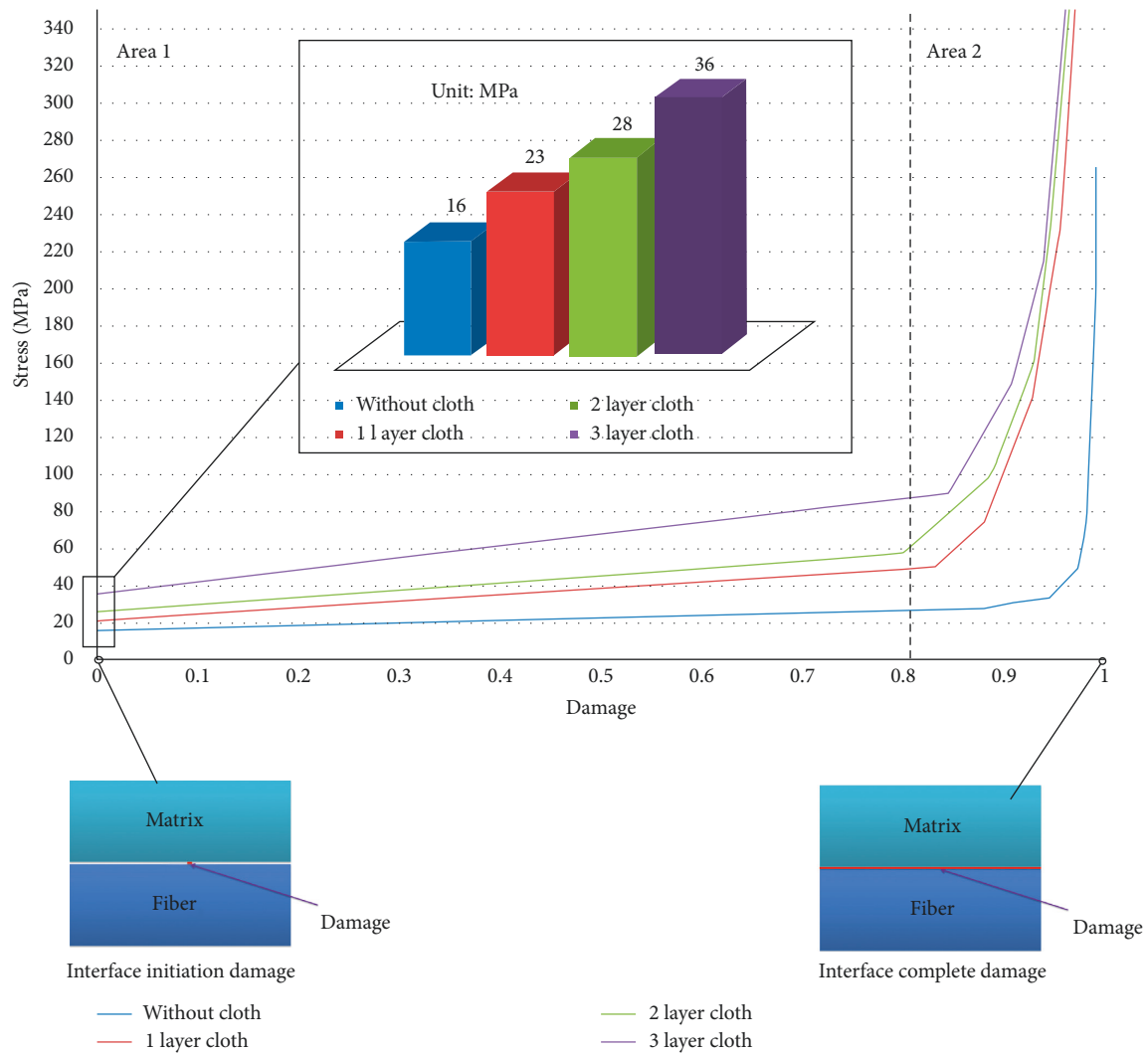


FIGURE 14: Comparison of stress versus damage.

unidirectional pultruded structure, and this method is implemented on the large smart composite platform. From the previous study [4–7], maximum stress near the bolt hole was around 75 MPa which was on ply-1 (Figure 15). After adding bidirectional fiberglass cloths to the large platform shell model, it is observed that the effect of stress concentration near the bolt hole had decreased to around 67 MPa in ply-1 (Figure 16). In this model, a maximum stress of 82 MPa was on bidirectional fiberglass cloth ply. Here, cloths act as a protective layer to the unidirectional fiberglass material from damage and decreased the stress from 75 MPa to 67 MPa. This result shows that there is an improvement in reduction of stress concentration effect on large smart composite platform, and this can enhance delamination strength.

**3.3. Comparison of Different Bidirectional Fiberglass Cloths.** To select an appropriate bidirectional fiberglass cloth material which can enhance delamination strength, numerical simulations were performed with three different densities

and results were plotted (Figure 17). They were selected considering the beam thickness of smart composite platform and industrial availability. The bidirectional fiberglass cloth with a weight of 186 g/m<sup>2</sup> and thickness of 0.14 mm has damage initiation stress around 41 MPa; the bidirectional fiberglass cloth with a weight of 295 g/m<sup>2</sup> and thickness of 0.23 mm has damage initiation stress around 49 MPa; and the bidirectional fiberglass cloth with a weight of 318 g/m<sup>2</sup> and thickness 0.28 mm has damage initiation stress around 59 MPa. The bidirectional fiberglass cloth with a weight of 318 g/m<sup>2</sup> and thickness of 0.28 mm which showed better performance in reducing damage has been selected for large smart composite platform.

In order to study the effect of number of wraps, different layers of bidirectional fiberglass cloths were wrapped on the micromechanical model and numerical simulations were performed. The results were plotted (Figure 18), and the damage initiation stress value after adding each layer was estimated. It was observed that after 3 layers of wrapping, damage initiation stress was saturating. Simulations were carried out up to 7 layers in order to estimate the variation in

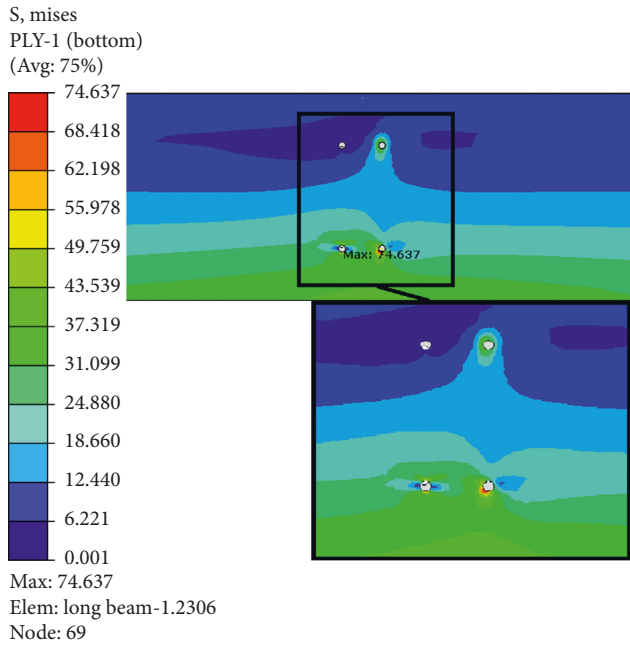


FIGURE 15: Stress contour plot around bolt for unidirectional pultruded composite platform before adding cloth.

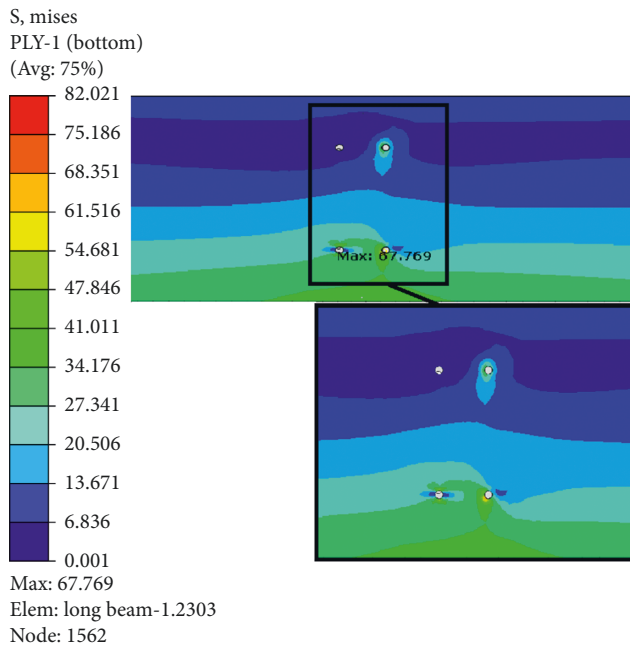


FIGURE 16: Stress contour plot around bolt for unidirectional pultruded composite platform after adding cloth.

stress values. Damage initiation stress was 35 MPa, 47 MPa, 59 MPa, 61 MPa, 63 MPa, 66 MPa, and 68 MPa from layer 1 to layer 7, respectively. From Figure 19, it is evident that layer 4, layer 5, layer 6, and layer 7 have very less improvement in damage initiation stress. The addition of more layers without obtaining better performance will increase the budget and the weight of the structure. Delamination failure will occur when the transverse shear load experienced will

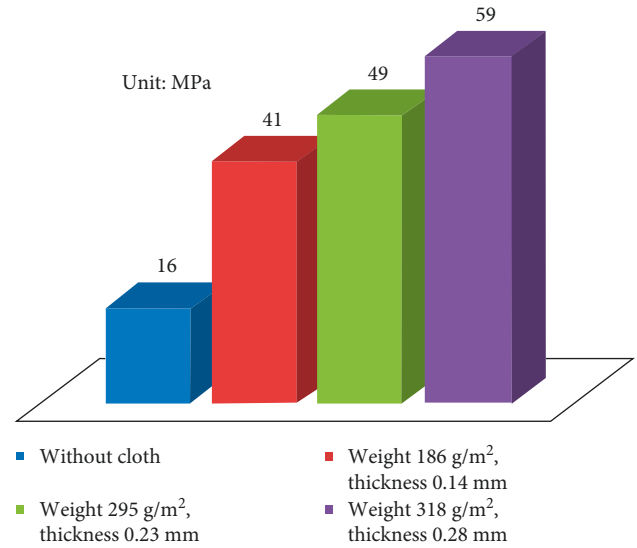


FIGURE 17: Comparison of damage initiation stress for different bidirectional fiberglass cloths with 3 layers.

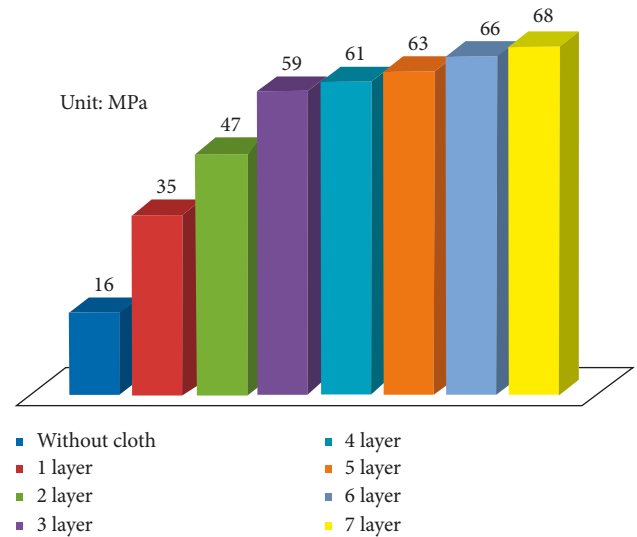


FIGURE 18: Comparison of damage initiation stress for 7 layers.

exceed interlaminar shear strength (ILSS) [26]. In Handbook of Adhesion [27], interlaminar shear strength (ILSS) for E-glass/vinylester was estimated as 51 MPa. As mentioned above, damage initiation stress for layer 3 is 59 MPa; that is, damage initiation stress for layer 3 is above interlaminar shear strength (ILSS) limit, and it can restrict delamination. So, the number of layers is selected as three.

**3.4. Comparison of Bidirectional Fiberglass Cloths and Conventional Continuous Fiberglass Mats.** Bidirectional fiberglass cloths have better mechanical properties compared to the conventional continuous fiberglass mat due to the proper orientation of fibres in both directions, whereas fibres are oriented randomly in mats (Figure 20). As the aim of this study is to decrease damage and increase delamination strength, a better material that can reinforce the structure

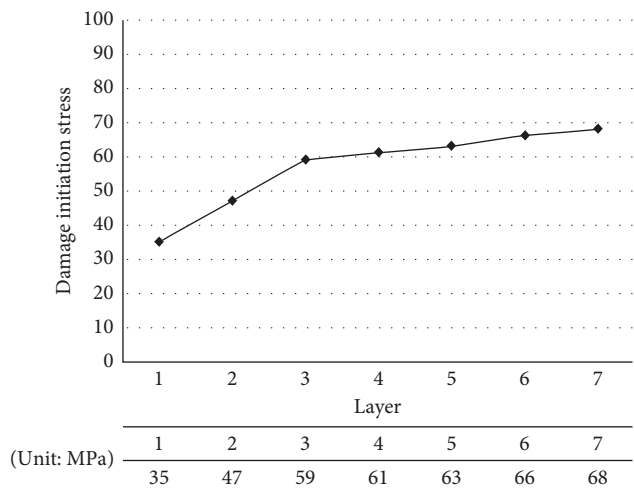


FIGURE 19: Damage initiation stress versus layer.

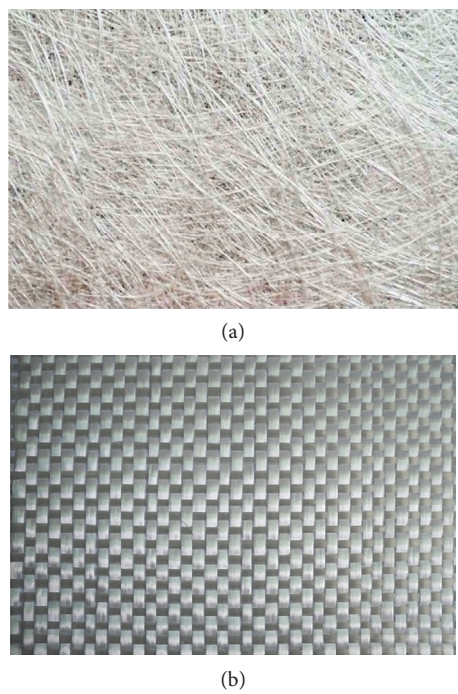


FIGURE 20: (a) Continuous fiberglass mat and (b) bidirectional fiberglass cloth.

will be a better choice. The quality of each mat from different industries is dissimilar, and as mentioned earlier, the applications of pultruded structures are mainly in civil engineering. So, selection of good quality material cloth is better compared to that of lower quality mat in order to avoid the risk of human life and increase safety. Moreover, from Figure 21, damage initiation stress for bidirectional fiberglass and continuous fiberglass mat are 59 MPa and 44 MPa, respectively. This difference shows that bidirectional fiberglass cloths have better properties in restricting delamination. Considering all these facts, bidirectional fiberglass cloths have better performance despite their cost compared to continuous fiberglass mats.

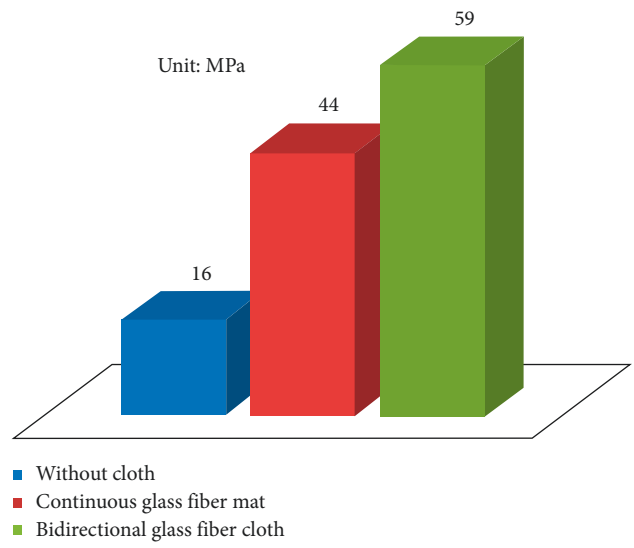


FIGURE 21: Comparison of the damage initiation stress for bi-directional fiberglass cloths and continuous fiberglass mats.

4. Conclusion

Unidirectional composites are subjected to delamination at very low stress, and these issues cannot be tolerated in some demanding applications. Most of the applications of pultruded structures are in civil engineering, which involves human safety. Therefore, it is essential to study the correlation of delamination onset and find a technology to enhance delamination strength as high as possible. The aim of this work was to enhance delamination strength of unidirectional pultruded large smart composite platforms. The micromechanical model of unidirectional pultruded composite was created, and different simulations were carried out in order to investigate defects. From the bibliography, it was found that debonding between fibre and matrix will occur before other defects, and this will lead to delamination. Bidirectional fiberglass cloth wrappings were used to prevent delamination, and different simulations were performed without wrapping cloths and with different layers of cloth wrapping. From a numerical simulation results, it was estimated that the bidirectional fiberglass cloth wrapping method was effective in preventing delamination. Due to the high cost of bidirectional fiberglass cloths, a study was also performed considering the number of layers and density to select an appropriate bidirectional fiberglass cloth material that can be considered as cost effective. After these studies, bidirectional fiberglass cloth with a weight of 318 g/m<sup>2</sup>, thickness of 0.28 mm, and 3 layers of wrap were selected. The result of a comparison study shows that bidirectional fiberglass cloths have better ability to restrict delamination compared to continuous fiberglass mats.

Data Availability

The data used to support the findings of this study are available from the corresponding author upon request.



## Conflicts of Interest

The authors declare that there are no conflicts of interest regarding the publication of this paper.

## References

- [1] M. Drissi-Habti, "Smart composite materials project DECID2 for structural applications," *JEC Composites*, vol. 42, pp. 28–29, 2008.
- [2] L. M. P. Durão, J. M. R. Tavares, V. H. C. De Albuquerque, J. F. S. Marques, and O. N. Andrade, "Drilling damage in composite material," *Materials*, vol. 7, no. 5, pp. 3802–3819, 2014.
- [3] L. M. P. Durão, D. J. S. Gonçalves, J. M. R. S. Tavares, V. H. C. de Albuquerque, and A. T. Marques, "Comparative analysis of drills for composite laminates," *Journal of Composite Materials*, vol. 46, no. 14, pp. 1649–1659, 2012.
- [4] X. Chapeleau, M. Drissi-Habti, and T. Tomiyama, "Embedded optical fiber sensors for in situ and continuous health monitoring of civil engineering structures in composite materials," *Materials Evaluation*, vol. 68, no. 4, pp. 409–415, 2010.
- [5] X. Chapeleau, M. Drissi-Habti, and T. Tomiyama, "Embedded optical fiber sensors for in situ and continuous health monitoring of composite materials in civil engineering structures," *Japan Society for Composite Materials*, vol. 36, no. 1, pp. 227–235, 2010.
- [6] A. Cordelle and M. Drissi-Habti, "Nanoindentation characterization of vinylester glass-fiber composites submitted to dense ultraviolet radiation exposure," *Materials Evaluation*, vol. 71, no. 4, 2013.
- [7] I. D. Madukauwa-David and M. Drissi-Habti, "Numerical simulation of the mechanical behavior of a large smart composite platform under static loads," *Composites Part B: Engineering*, vol. 88, pp. 19–25, 2016.
- [8] P. Carlone, G. Salvatore Palazzo, and R. Pasquino, "Pultrusion manufacturing process development by computational modelling and methods," *Mathematical and Computer Modelling*, vol. 44, no. 7, pp. 701–709, 2006.
- [9] Creative Pultrusions, *Composite Sheet Pile Wall System*, Creative Pultrusions, Pleasantville, PA, USA, 2016, <http://www.creativepultrusions.com/index.cfm/fiberglass-pultruded-systems/composite-sheet-pile-system>.
- [10] G. Ginger, *Rail Line Landmark Restoration via Pultrusion*, CompositesWorld, Scottsdale, AZ, USA, 2016, <http://www.compositesworld.com/articles/rail-line-landmark-restoration-via-pultrusion->.
- [11] M. U. Farooq, L. A. Carlsson, and B. A. Acha, "Determination of fiber/matrix adhesion using the Outwater–Murphy single fiber specimen," *Engineering Fracture Mechanics*, vol. 76, no. 18, pp. 2758–2765, 2009.
- [12] M. S. Kumar, K. Raghavendra, M. A. Venkataswamy, and H. V. Ramachandra, "Fractographic analysis of tensile failures of aerospace grade composites," *Materials Research*, vol. 15, no. 6, pp. 990–997, 2012.
- [13] Y. Bai, T. Vallée, and T. Keller, "Delamination of pultruded glass fiber-reinforced polymer composites subjected to axial compression," *Composite Structures*, vol. 91, no. 1, pp. 66–73, 2009.
- [14] DuraGrid, *DURAGRID® Benefits*, 2016, <http://www.prmetals.com/Product/Grating/Fiberglass-Grating/Pultruded-Fiberglass-Grating/DURADEK/DURADEK-I6000-Pultruded-Grating-112-Depth>.
- [15] R. Karakuzu, T. Gülem, and B. M. İçten, "Failure analysis of woven laminated glass–vinylester composites with pin-loaded hole," *Composite Structures*, vol. 72, no. 1, pp. 27–32, 2006.
- [16] A. Shukla, Y. D. Rajapakse, and M. E. Hynes, *Blast Mitigation: Experimental and Numerical Studies*, Springer Science & Business Media, Berlin, Germany, 2013.
- [17] ABAQUS, *Abaqus 6.10 Analysis User's Manual, Volume V: Prescribed Conditions, Constraints & Interactions. 33.1.10 Surface-Based Cohesive Behavior*, 2016, [http://abaqusdoc.ugalaxy.ca/pdf\\_books/ANALYSIS\\_5.pdf](http://abaqusdoc.ugalaxy.ca/pdf_books/ANALYSIS_5.pdf).
- [18] W. G. Jiang, R. Z. Zhong, Q. H. Qin, and Y. G. Tong, "Homogenized finite element analysis on effective elastoplastic mechanical behaviors of composite with imperfect interfaces," *International Journal of Molecular Sciences*, vol. 15, no. 12, pp. 23389–23407, 2014.
- [19] A. M. G. Coelho, J. T. Mottram, and N. Matharu, "Virtual characterization of delamination failures in pultruded GFRP angles," *Composites Part B: Engineering*, vol. 90, pp. 212–222, 2016.
- [20] M. Knops, *Analysis of Failure in Fiber Polymer Laminates: The Theory of Alfred Puck*, Springer Science & Business Media, Berlin, Germany, 2008.
- [21] A. Puck and H. Schürmann, "Failure analysis of FRP laminates by means of physically based phenomenological models," *Composites Science and Technology*, vol. 62, no. 12–13, pp. 1633–1662, 2002.
- [22] J. Qureshi, J. T. Mottram, and B. Zafari, "Robustness of simple joints in pultruded FRP frames," *Structures*, vol. 3, pp. 120–129, 2015.
- [23] P. P. Camanho, C. G. Davila, and M. F. De Moura, "Numerical simulation of mixed-mode progressive delamination in composite materials," *Journal of Composite Materials*, vol. 37, no. 16, pp. 1415–1438, 2003.
- [24] A. M. G. Coelho, "Finite element guidelines for simulation of delamination dominated failures in composite materials validated by case studies," *Archives of Computational Methods in Engineering*, vol. 23, no. 2, pp. 363–388, 2016.
- [25] HexForce, *Hexcel Technical Fabrics Handbook*, HexForce, Stamford, CT, USA, 2016, [http://www.hexcel.com/Resources/DataSheets/Brochure-Data-Sheets/HexForce\\_Technical\\_Fabrics\\_Handbook.pdf](http://www.hexcel.com/Resources/DataSheets/Brochure-Data-Sheets/HexForce_Technical_Fabrics_Handbook.pdf).
- [26] Z. Fan, M. H. Santare, and S. G. Advani, "Interlaminar shear strength of glass fiber reinforced epoxy composites enhanced with multi-walled carbon nanotubes," *Composites Part A: Applied Science and Manufacturing*, vol. 39, no. 3, pp. 540–554, 2008.
- [27] D. E. Packham, *Handbook of Adhesion*, John Wiley & Sons, Hoboken, NJ, USA, 2006.

